行政院國家科學委員會專題研究計畫　期中進度報告

沿薄膜管中調節流體速度以提高超過濾效率(1/2)

計畫類別：個別型計畫
計畫編號：NSC94-2214-E-032-005-
執行期間：94 年 08 月 01 日至 95 年 10 月 31 日
執行單位：淡江大學化學工程與材料工程學系

計畫主持人：葉和明

報告類型：精簡報告
報告附件：出席國際會議研究心得報告及發表論文
處理方式：本計畫可公開查詢

中　華　民　國 95 年 4 月 21 日

The effect of hydraulic behavior on ultrafiltration in a membrane tube inserted concentrically with a solid rod of linearly varied rod radius

Ho-Ming Yeh*

Department of Chemical and Material Engineering, Tamkang University

Tamsui, Taipei County, Taiwan 251, ROC

Abstract

Increasing the fluid velocity in cross-flow membrane ultrafilter has two conflict effects. One, the decrease in concentration-polarization resistance, is good for ultrafiltration, while the other, the decrease in average transmembrane pressure, is bed for performance. Since along the flow channel of a cross-flow membrane ultrafiltration, the concentration-polarization increases while the transmembrane pressure decreases. Therefore, proper adjusment of the convection strength along the flow channel might effectively suppress the undesirable concentration-polarization resistance while still preserving an effective transmembrane pressure, and thereby lead to improved permeate recoveries. In present study, the effect of hydraulic behavior on membrane ultrafiltration in a tubular module inserted concentrically with a steed rod wrapped by a wire spiral with wire angle varied along the flow channel, was investigated and the appropriate manner of wire-angle variation along the tube was discussed. It is concluded that for the modules of fixed average wire-spiral angle, the best manner of wire-angle variation is such that the wire angle should increase gradually from 0^o along the flow channel.

Keywords: Ultrafiltration, Wire-rod tubular membrane, Spiral wire, Angle variation

* Corresponding author. Fax: +886-22620-9887

E-mail address: hmyeh@mail.tku.edu.tw (H. M.Yeh)

1. Introduction

Ultrafiltration is primarily a siz-exclusion-based pressure-driven membrane separation process, the pressure applied to the working fluid provides the driving potential to force the solvent to flow through the membrane. Although, separation by ultrafiltration is mainly based on relative molecular sizes, the chemistry of the solute membrane interaction is also important. The molecular weight cutoff (MWCO) of any given membrane can vary with changing feed chemistries as well as with factors such as molecular orientation, molecular configuration, operation conditions. etc.[1].

Ultrafiltration of macromolecular solutions has become an increasingly important separation process. Today, the following applications have been proven to be economically attractive and useful [2,3]: industrial effluents, oil emulsions, wastewater, biological macromolecules, colloidal paint suspensions and medical therapeutics. The transmembrane pressure applied is usually in the range of 10 to 100 psi. The rapid development of this process was made possible by the advent of anisotropic, high-flux membranes capable of distinguishing among molecular and colloidal species in the 0.001 to 10 μm size range.

The advantage of ultrafiltration as compared to other dewatering processes, such as evaporation and freezing, is the absence of a change in phase or state of the solvent. Evaporation requires the input of about 1000 Btu/lb of water evaporated while freezing requires about 144 Btu/lb of water frozen, merely to effect the change of water from liquid to vapor and liquid to solid, respectively. A less obvious advantage is the fact that no complicated heat-transfer or heat-generating equipment is needed, only electrical energy to drive the pump motor is required.

In cross-flow ultrafiltration the permeate flux generally declines with filtration time due to the phenomenon of concentration polarization by the rejected particles [4-6]. Several hydraulic approaches developed for reducing the effects of

concentration polarization and progressive fouling to enhance the permeate flux, have been discussed thoroughly [7-17]. The use of inserts, such as metal grills [7], static rods [8], spiral wire [9], disc and doughnut shape inserts [10] and helical baffles [11], in a tubular membrane have been tried to different membrane processes. Da Costa et al. performed an extensive study of ultrafiltration flux by net-type spacers [12-14]. The applications of combined [15] and multipass [16] systems in hollow-fiber modules were also reported.

The enhancements of performance for ultrafiltration in tubular membranes with a steel rod inserted [17] and with a twisted wire-rod assembly [18] were investigated in previous works. In the previous study of twisted wire-rod modules, only the constant angle of wire spiral through the flow channel were considered. For more detailed study of the hydraulic behavior in these modules, the effect of the variation of wire angle along the flow channel on performance will be investigated in present work.

2. Wire-rod membrane module with wire angle varied

It was found that the performance of ultrafiltration in the tubular membrane could be improved by inserting concentrically a steel rod, resulting in increased fluid velocity, and that the performance would be further improved if the steel rod was wrapped entirely with a helical wire[17,18]. Actually, rising fluid velocity in the cross-flow type membrane modules has two conflict effects on ultrafiltration. One, the decrease in resistance to permeation due to reduction in concentration polarization, is good for ultratfiltration, while the other, the decrease in average transmembrane pressure due to increase in frictional pressure loss, is bad for ultrafiltration. It appear, therefore, that proper adjustment of fluid velocity distribution along the flow channel as well as propor arrangement of the profile of flow channel with a specified volumetric feed rate, might effectively suppress any undesirable resistance to

permeation due to concentration polarization while still preserving an effective transmembrane pressure, and thereby lead to improved permeate recoveries.

Consider a modified tubular-membrane module of radius r_m inserted concentrically with a steel rod of radius kr_m, on which a tight fitting wire spiral of varied angle, having a diameter nearly equal to the annular spacing, is wrapped entirely on the steel rod as a spacer, as shown in Fig. 1. Acutally, the modified module shown in Fig. 1 is exactly the same as that employed in previous works [18], except that the wire angle, instead of being unchanged, varies gradually along the flow channel. In present study, we will investigate the effect of wire-angle variation, either increasing or decreasing along the flow channel, on the reduction of concentration–polarization resistance and transmembrane pressure.

3. Resistance-in-series model

Recently, new theoretical modeling was carried out in detail at the University of Bath, UK [19,20]. Further, Song and Elimelech [21] developed the fundamental theory and methodology providing a solid basis for the study of limiting flux in ultrafiltration. Later, a mechanistic model for predicting the limiting flux in ultrafiltration was also developed [22].

However, membrane ultrafiltration of macromolecular solutions is usually analyzed by the following models: (1) the gel polarization model [23-29], (2) the osmotic pressure model [30-38], and the resistance-in-series model [39-41]. In the gel polarization model, permeate flux is reduced by the hydraulic resistance of gel layer. In the osmotic pressure model, permeate flux reduction results from the decrease in effective transmembrane pressure that occurs as the osmotic pressure of the retentate increases. In resistance-in series model, permeate flux decreases due to the resistances caused by fouling or solute adsorption and

concentration polarization. Among them the last model more easily describes the relationships of permeate flux with operating parameters.

In the resistance-in-series model, permeate flux $J(z)$ may be expressed as

$$J(z) = \frac{\Delta P(z)}{R_m + R_f + R_p} \tag{1}$$

where R_m denotes the intrinsic resistance of a membrane, and R_p and R_f, respectively, are the resistances due to the concentration polarization/gel layer and those due to other fouling phenomena such as solute adsorption, while ΔP is the transmembrane pressure defined as

$$\Delta P(z) = P(z) - P_p \tag{2}$$

In above equation, $\Delta P(z)$ is the pressure distribution of tube side along the flow channel and P_p is the permeate pressure of the shell side which may be assumed to be constant.

R_p will be proportional to the amount and specific hydraulic resistance of the deposited layer. Since the deposite layer is compressible, R_p is function of pressure, so that we may assume, with ϕ as the proportional constant

$$R_p = \phi \Delta P(z) \tag{3}$$

and Eq.(1) becomes

$$J(z) = \frac{\Delta P(z)}{R_m + R_f + \phi \Delta P(z)} \tag{4}$$

As mentional earlier, membrane ultrafiltration is a pressure-driven separation, the pressure applied to the working fluid provides the driving potential to force the permeate to flow through the membrane. For a small

applied pressure, the permeate flux through a membrane is observed to be proportional to the applied pressure. However, as the pressure is increased, the flux begins to drop below that which would result from a linear flux-pressure behavior. Eventually, a limiting flux is reached where any further pressure increase no longer results in any increase in flux. Accordingly, the following conditions are reached:

for $\Delta P = 0,\ J = 0;$ (5)

for small $\Delta P,\ J = (const)\Delta P;$ (6)

as $\Delta P \to \infty$ (or large enough), $J = J_{\lim}$ (limiting flux) (7)

It is easy to show that Eqs. (5)-(7) satisfy Eq. (4), and that resistance-in-series model is not only easy to describle the phenomenon of ultrafiltration in the membrane module but also meets the required conditions during operation.

4. Experimental

The experimental apparatus, materials and procedure were exactly the same as those in previous work [18], except that the spiral wires of gradually varied angle along the flow channel were employed, as shown in Fig. 1. The membrane medium used in the wired module was mainly a 150 kDa MWCO tubular ceramic membrane (M2 type, Techsep, France; length L= 0.4m, i.d. $2r_m$= 6mm) with a steel rod of radius, kr_m= 2mm (k=2/3), inserted concentrically. A tight fitting wire spiral having the diameter nearly equal to the annular spacing, $(1-k)r_m$= 1mm, was wrapped with the wire angle varied on the entire steel rod as a spacer in the annulus.

Since the result that the best inclined angle of wire spiral was 30^o for the system of present interest was obtained in previous work [18], the following variation manners of wire angle θ were employed in present study: $30^o \to 20^o$, $30^o \to 10^o$, 30^o

$\rightarrow 0^o$, $0^o \rightarrow 30^o$, $10^o \rightarrow 30^o$, $20^o \rightarrow 30^o$. The experiment was also conducted with the wire angles of $0^o \rightarrow 0^o$ (without wire spiral) and $30^o \rightarrow 30^o$, as well as with k=0 (without steel rod), for comparison. To apply the wire, the desired spacing for the specified wire angles varied gradually were marked first on the steel rod. The wire was then wrapped in a spiral manner on the entire rod and finally fastened to the rod by small amounts of epoxy glue to attempt filling up the clearence (0.001 mm) between the membrane surface and helical wire.

The tested solute was dextran T500(Pharmacia Co., Sweden) which was more than 99% retained by the membrane used, while the solvent was distillated water. The feed solution concentrations C_i were 0.1, 0.2, 0.5 and 1.0 wt% dextran T500. Fig.2 shows the schematic diagram of experimental apparatus. The feed solution was circulated by a high-pressure pump with a variable speed motor (L-07553-20, Cole Parmer Co.), and the feed flow rates Q_i were controlled by a flowmeter (IR-OPFLOW 502-111, Headland Co.) to be 1.67, 2.50, 3.33 and 4.17 cm^3/s. The pressure at the inlet (P_i) and outlet (P_L) of the conduit as well as at shell side (P_p) were measured with a pressure transmitter (Model 891.14.425, Wika Co). The inlet transmembrane pressures ΔP_i were 30,50,80,110 and 140kPa. In all experiments the feed solution temperature was controlled as 25℃ by thermostat. The experimental procedure was follows. First, the permeate fluxes of liquid solution at psedudo steady state were measured in the tubular membrane. Next, continuous operations was conucted with a steel rod of radius $kr_m = 2\times10^{-3}$m (k=2/3) inserted concentrically in the membrane tube. Finally, the experimental results were also obtained in such a concentric-tube membrane module with a helical wire of varied angle.

5. Results and discussion

5.1. Permeate fluxes

Many experimental results of average permeate fluxes, $\overline{J}$, were obtained [42], and some of them are plotted in Figs. 3-6, It is seen from these figures that the order of magnitude for averaged permeate flux obtained in the following devices is

wire-rod module ($k > 0$, $\theta > 0$) > wire-free rod module ($k > 0$, $\theta = 0$) > rod-free module ($k = 0$, $\theta = 0$) (8)

Further, among the wire-rod modules

($0^o \rightarrow 30^o$) module >($30^o \rightarrow 0^o$) module >($10^o \rightarrow 30^o$) module >($30^o \rightarrow 10^o$) module >($20^o \rightarrow 30^o$) module >($30^o \rightarrow 20^o$) module >($30^o \rightarrow 30^o$) module (9)

5.2. Effect of steel rod and wire spiral on permeate flux

The fact of Eq.(8) was already verified in previous works [17, 18]. It was reported in these studies that increasing fluid velocity in the tubular-membrane ultrafiltration module by inserting concentrically a steel rod could reduce the concentration-polarization layer, resulting in improved performance. Further, when the steel was wrapped entirely with a tight fitting wire spiral, having a dimeter nearly equal to the annular spacing, the flow section was further reduced, resulting in larger increase of flow velocity as well as permeate flux.

5.3. Effect of the variation of wire angle on permeate flux

Actually, increasing fluid velocity in the cross-flow type membrane modules has two conflict effects on ultrafiltration. One, the decrease in resistance to permeation due to reduction in concentration polarization, is good for ultrafiltration, while the other, the decrease in average transmembrane pressure due to increase in frictional pressure loss, is bad for ultrafiltration. Therefore, proper adjustment of the variation of

fluid velocity along the flow channel with a specified volumetric feed rate, might effectively suppress any undesirable resistance to permeation due to concentration polarization while still preserving an effective transmembrane pressure, and thereby lead to improved permeate recoveries. This fact is verified by Eq.(9) and will be further described as follows.

Since the thickness of concentration-polarizatino layer increases along the cross-flow channel, the smaller inclined angle of wire spiral, as well as less increment in fluid velocity, around the inlet region is sufficient enough to reduce the lower concentration-polarization resistance, while still preserving the effective transmembrane pressure. Accordingly, the order of magnitude for average permeate fluxes obtained in the following modules is

$(0^o \rightarrow 30^o)$ module $>(10^o \rightarrow 30^o)$ module $>(20^o \rightarrow 30^o)$module (10)

On the other hand, larger inclined angle of wire spiral, as well as higher speed of flowing fluid, around the outlet region is greatly required for suppressing the higher concentration-polarization layer, therefore

$(0^o \rightarrow 30^o)$ module $>(30^o \rightarrow 0^o)$ module (11)

$(10^o \rightarrow 30^o)$ module $>(30^o \rightarrow 10^o)$ module (12)

$(20^o \rightarrow 30^o)$ module $>(30^o \rightarrow 20^o)$ module (13)

Further, in the modules of high inlet wire angle (say 30^o), since the transmembrane pressure were largely reduced in the front of the flow channel, further maintaining a certain degree of wire angle around the outlet region for suppressing the higher concentration-polarization resistance there cannot compensate with the further decrease of transmembrane pressure. Thus

$(30^o \rightarrow 0^o)$ module $>(30^o \rightarrow 10^o)$ module $>(30^o \rightarrow 20^o)$ module $>(30^o \rightarrow 30^o)$ module (14)

Finally, it is readily to see from Figs. 3-6 that

($30^o \rightarrow 0^o$) module >($10^o \rightarrow 30^o$) module (15)

($30^o \rightarrow 10^o$) module >($20^o \rightarrow 30^o$) module (16)

($30^o \rightarrow 20^o$) module >($30^o \rightarrow 30^o$) module (17)

This result indicates that the order of performance in wire-rod tubular membranes with wire angle varied gradually is

Module with $\bar{\theta}=15^o$ > module with $\bar{\theta}=20^o$ > module with $\bar{\theta}=25^o$ > module with $\bar{\theta}=30^o$ (18)

5.4. Effect of the variation of wire angle on resistances

If experimental data obtained in membrane ultrafiltration is applied to Eq. (4), then the following relation of the average experimental values is reached

$$\left(\bar{J}\right)_{\text{exp}} = \frac{\left(\overline{\Delta P}\right)_{\text{exp}}}{R_m + R_f + \phi\left(\overline{\Delta P}\right)_{\text{exp}}} \tag{19}$$

or

$$\frac{1}{\left(\bar{J}\right)_{\text{exp}}} = \phi + \frac{R_m + R_f}{\left(\overline{\Delta P}\right)_{\text{exp}}} \tag{20}$$

Therefore, from a straight line plot of $1/\left(\bar{J}\right)_{\text{exp}}$ versus $1/\left(\overline{\Delta P}\right)_{\text{exp}}$ under certain operating conditions, Q_i and C_i, the values of ϕ (the intersection at ordinate) and $\left(R_m + R_f\right)$(the slope) may be determined experimentally [15-18]. With the use of experimental data and Eq.(20) the intersection at ordinate, ϕ, and the slope of this straight line, $\left(R_m + R_f\right)$, were determined [42].

Some values of ϕ and $\left(R_m + R_f\right)$ determined are listed in Tables 1 and 2. It is found from these tables that the validity of the result of Sections 5.1-5.3 is readly confirmed because the orders of magnitude for the resistance of permeation, ϕ and $\left(R_m + R_f\right)$, are in the opposite directions to those for permeate flux in Eqs. (8)-(18).

Conclusion

The effect of hydraulic behavior on membrane ultrafiltration in the wire-rod tubular module has been investigated by varying the wire spiral angle along the flow channel. Increasing the wire spiral angle will reduce the cross section of flow channel, as well as increase the fluid velocity. Actually, rising the fluid velocity in the flow channel of a cross-flow membrane ultrafilter has two conflict effects, the desirable effect of decreasing concentration-polarization layer and the undesirable effect of decreasing transmembrane pressure. Along the flow channel of a wire-rod tubular membrane, the concentration-polarization resistance increases while the trans-membrane pressure decreases. It is concluded that for the devices of same average wire-spiral angle $\overline{\theta}$, the best manner of wire-angle variation is such that the wire angle should increase gradually from 0^o along the flow channel, while for the modules of different average values of wire angle, $\overline{\theta}$, the order of performance within the operating conditions of present interest is : ($\overline{\theta} = 15^o$) >($\overline{\theta} = 20^o$) >($\overline{\theta} = 25^o$) >($\overline{\theta} = 30^o$).

Acknowledgements

The authors wish to express their thanks to the National Science Council of ROC for financial aid with the Grant No. NSC 89-2214-E-032-009.

References

[1] S. S. Kulkarni, E.W. Funk an N. N. Li, Ultrafiltration, in W. S. W. Ho and K. K. Sirkar (Eds.), Membrane Handbook, Chapman and Hall, New York, 1992, p393.

[2] M. C. Porter, Membrane filtration, in P. A. Schweitzer (Ed.), Handbook of Separation Techniques for Chemical Engineers, McGraw-Hill, New York, 1979,

Sect. 2.1.

[3] M. Cheryan, Ultrafiltration, Handbook, Technomic Publiching Co. Inc., Lancaster, Pennsylvania, 1986, Sect. 8.

[4] S. Nokao, T. Nomura and S. Kimura, Characteristics of Macromolecular gel layer formed on ultrafiltration tubular membrane, AIChE J., 25 (1979) 615.

[5] A. G. Fane, C. J. D. Fell and A. G. Waters, The relationship between membrane surface pore characteristics and flux for ultrafiltration membrnes, J. Member. Sci. , 9(1981) 245.

[6] M. J. Clifton, N. Abidine, P. Aptel and V. Sanchez, Growth of the polarization layer in ultrafiltration with hollow-fiber membranes, J. Membr. Sci., 21 (1984) 233.

[7] D. C. Thomas, Enhancement of forced convection heat transfer coefficient using detached turbulence promoters, Ind. Eng. Chem. Process Design Dev.,6 (1967) 385.

[8] C. Peri and W. L. Dunkley, Reverse osmosis of cotlage cheese whey, Influence of flow conditions, J. Food Sci., 36 (1971) 395.

[9] S. Poyen, F. Quemeneur and B. Bariou, Improvement of the flux of permeate in ultrafiltration by turbulence promoters, Int. Chem. Eng., 27 (1987) 441.

[10] J. A. Howell, R. W. Field and Dengxi Wu, Yeast cell microfiltration: Flux enhancement in baffled and pulsatill flow system, J. Membr. Sci., 80 (1993) 59.

[11] B. B. Gupta, J. A. Howell, D. Wu and R. W. Field, A helical baffle for cross- flow microfiltration, J. Membr. Sci., 99 (1995) 31.

[12] A. R. Da Costa, A. G. Fane, C. J. D. Fell and A. C. M. Franker, Optimal channel spacer design for ultrafiltration, J. Membr. Sci., 62 (1991) 275

[13] A. R. Da Costa, A. G. Fane and D. E. Wiley, Spacer charaterization and pressure drop modulling in Spacer-filled channels for ultrafiltration, J. Membr. Sci., 87

(1994) 79

[14] A. R. Da Costa, A. G. Fane, Net-type spacers: Effect of configuration on fluid flow path and ultrafiltration flux, Ind. Eng. Chem. Res., 33 (1994) 1845

[15] H. M. Yeh and H. H. Wu, Membrane ultrafiltration in combined hollow-fiber module systems, J. Membr. Sci., 124 (1997) 93.

[16] H. M. Yeh and J. W. Tsai, Membrane ultrafiltration in multipass hollow-fiber modules, J. Membr. Sci., 142 (1998) 61.

[17] H. M. Yeh, H.Y. Chen and K.T. Chen, Membrane ultrafiltration in a tubular module with a steel rod inserted concentrically for improved performance, J. Membr. Sci., 168 (2000) 121.

[18] H. M. Yeh, K. T. Chen, Improvement of ultrafiltration performance in tubular membranes using a twisted wire-rod assembly, J. Membr. Sci. 178 (2000) 43.

[19] J. A. Howell, Subcritical flux operation of microfiltration, J. Membr. Sci. 107 (1955) 165.

[20] D. X. Wu, J. A. Howell, R. Fired, Critical flux measurement for model colloids, J. Membr. Sci. 152 (1999) 89.

[21] L. Song, M. Elimelech, Theory of concentration polarization in crossflow filtration, J. Chem. Soc. Faraday Trans. 91 (1995) 3389.

[22] L. Song, A new model for the calculation of the limiting flux in ultrafiltration, J. Membr. Sci., 144 (1998) 173.

[23] W.F. Blatt, A. Dravid, A.S. Michales and L. Nelsen, Solute polarization and cake formation in membrane ultrafiltration: causes, consequences, and control techniques, in J.E. Filnn (Ed.), Membrane Science and Technology, Plenum Press, New York, 1970, p. 47.

[24] M.C. Porter, Concentration polarization with membrane ultrafiltration, Ind. Eng. Chem. Proc. Res. Dev., 11(1972)234.

[25] R.B. Grieves, D. Bhattacharyya, W.G. Schomp and J.L. Bewley, Membrane ultrafiltration of a nonionic surfactant, AIChE J., 19(1973)766.

[26] J.J.S. Shen and R.F. Probstein, On the prediction of limiting flux in laminar ultrafiltration of macromolecular solutions, Ind. Eng. Chem. Fundam., 16(1977)459

[27] S. Nakao, T. Nomura and S. Kimura, Characteristics of Macromolecular gel layer formed on ultrafiltration tubular membrane, AIChE J., 25(1979)615.

[28] A.G. Fane, C.J.D. Fell and A.G. Waters, The relarionship between membrane surface pore characteristics and flux for ultrafiltration membranes, J. Membr. Sci., 9(1981)245

[29] A.G. Fane, Ultrafiltration of suspensions, J. Membr. Sci. 20(1984)249

[30] J.G. Wijmans, S. Nakao and C.A. Smolders, Flux limitation in ultrafiltration: osmotic pressure model and gel layer model, J. Membr. Sci. 20(1984)115.

[31] A.A. Kozinki and E.N. Lightfoot, Protein ultrafiltration: a general example of boundary layer filtration, AIChE J., 18(1972)1030.

[32] W. Leung and R.F. Probstein, Low polarization in laminar ultrafiltration of macromolecular solutions, Ind. Eng. Chem. Fundam., 18(1979)274.

[33] R.P. Wendt, E. Klein, F.F. Holland and K.E. Eberle, Hollow fiber ultrafiltration of calf serum and albumin in the Pregel uniform-wall-flux region, Chem. Eng. Commun., 8(1981)251.

[34] S. Nakao and S. Kimura, Model of membrane transport phenomena and their applications for ultrafilration data, J. Chem. Eng. Jpn., 15(1982)200.

[35] C. Kleinstreuer and M.S. Paller, Laminear dilute suspension flows in plate - and-frame ultrafiltration units, AIChE J., 29(1983)529.

[36] M.J. Clifton, N. Abidine, P. Aptel and V. Sanchez, Growth of the polarization layer in ultrafiltration with hollow-fiber membrane, J. Membr. Sci., 21(1984)233.

[37] R.P. Gooding Ma, C.H. Gooding and W.K. Alexander, Adynamic model for low-pressure, hollow-fiber ultrafiltration, AIChE J., 31(1985)1782.

[38] H. Nabetani, M. Nakajima, A. Watanable, S. Nakao and S. Kumura, Effects of osmotic pressure and adsorption on ultrafiltration of ovalbumin, AIChE J., 36(1990)907.

[39] B.H. Chiang and M. Cheryan, Ultrafiltration on skim milk in hollow fibers, J. Food Sci., 51(1986)340.

[40] M. Assadi and D.A. White, A model for determining the steady state flux of inorganic microfiltration membrane, Chem. Eng. J., 48(1992)11.

[41] H.M. Yeh and T.W. Cheng, Resistance-in-series for membrane ultrafiltration in hollow fiber of tube-and-shell arrangement, Sep. Sci. Technol., 28(1993)1341.

[42] T.C. Liu, Improvement in permeate flux by varying the angle of wire spiral through wire-rod membrane modules, M.S. Thesis, Tamkang University, Tamsui, Taiwan, ROC, 2002.

Figure Legends

Fig.1. Schematic diagram of a wire-rod tubular-membrane module with wire angle varied gradually

Fig.2. Experimental apparatus

Fig.3. Average permeate flux vs. transmembrane pressure for $Q_i = 2.5\times10^{-6}$ m^3/s and $C_i = 0.1$ wt%.

Fig.4. Average permeate flux vs. transmembrane pressure for $Q_i = 4.17\times10^{-6}$ m^3/s and $C_i = 0.1$ wt%.

Fig.5. Average permeate flux vs. transmembrane pressure for $Q_i = 2.5\times10^{-6}$ m^3/s and $C_i = 1.0$ wt%.

Fig.6. Average permeate flux vs. transmembrane pressure for $Q_i = 4.17\times10^{-6}$ m^3/s and $C_i = 0.1$ wt%.

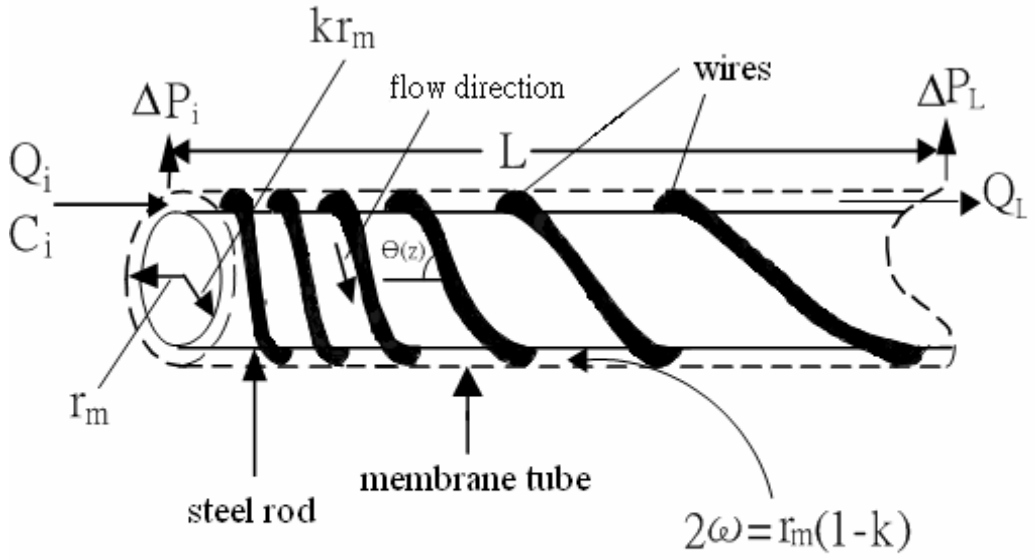
kr_m
ΔP_i
flow direction
wires
ΔP_L
L
Q_i
C_i
Q_L
θ(z)
r_m
steel rod
membrane tube
$2\omega = r_m(1-k)$

Fig.1

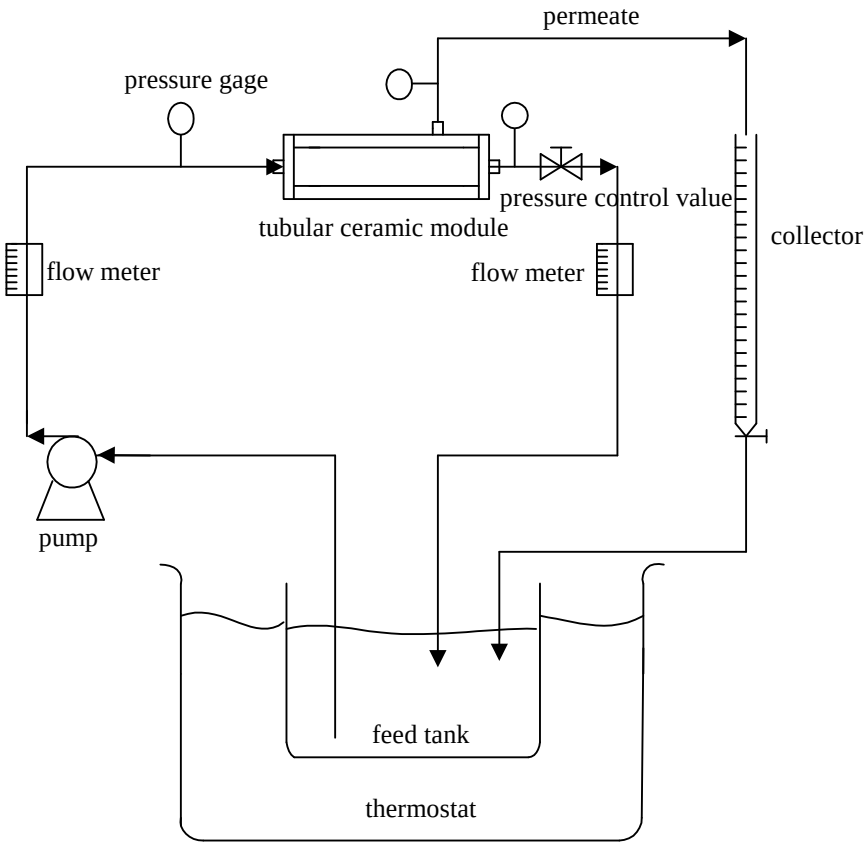
permeate
pressure gage
pressure control value
tubular ceramic module
collector
flow meter
flow meter
pump
feed tank
thermostat

Fig. 2

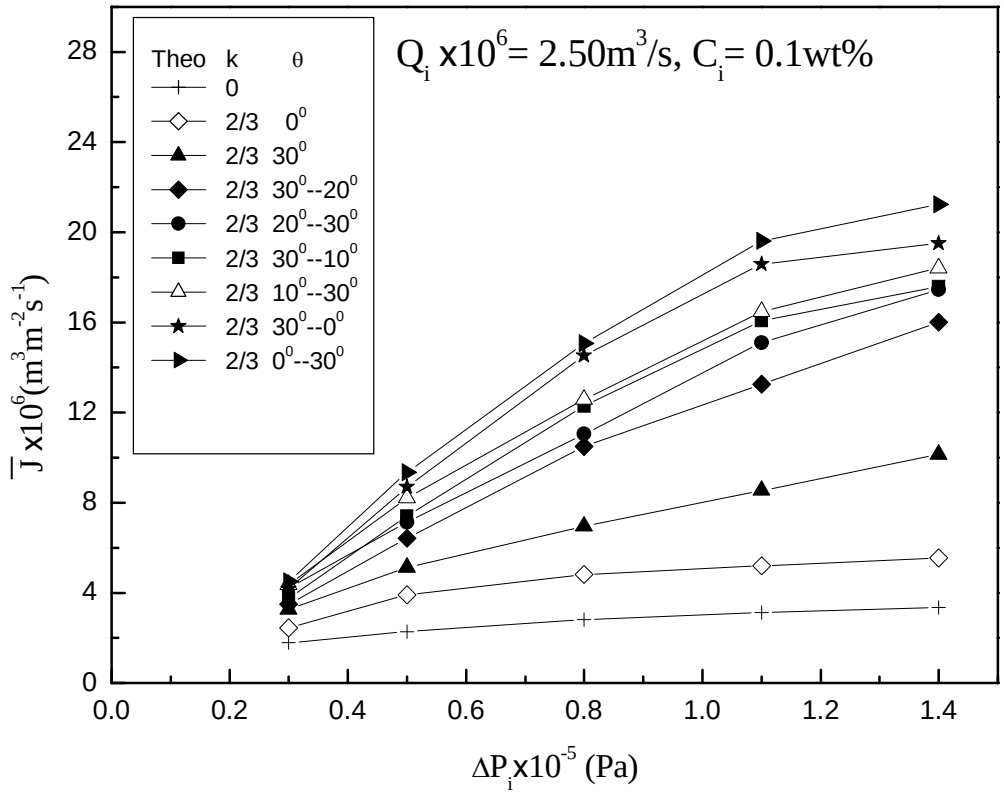
Theo k θ
0
2/3 0⁰
2/3 30⁰
2/3 30⁰--20⁰
2/3 20⁰--30⁰
2/3 30⁰--10⁰
2/3 10⁰--30⁰
2/3 30⁰--0⁰
2/3 0⁰--30⁰
Q_i x10^6= 2.50m^3/s, C_i= 0.1wt%
J̄ x10^6(m^3m^-2s^-1)
ΔP_i x10^-5 (Pa)
0
4
8
12
16
20
24
28
0.0
0.2
0.4
0.6
0.8
1.0
1.2
1.4

Fig.3

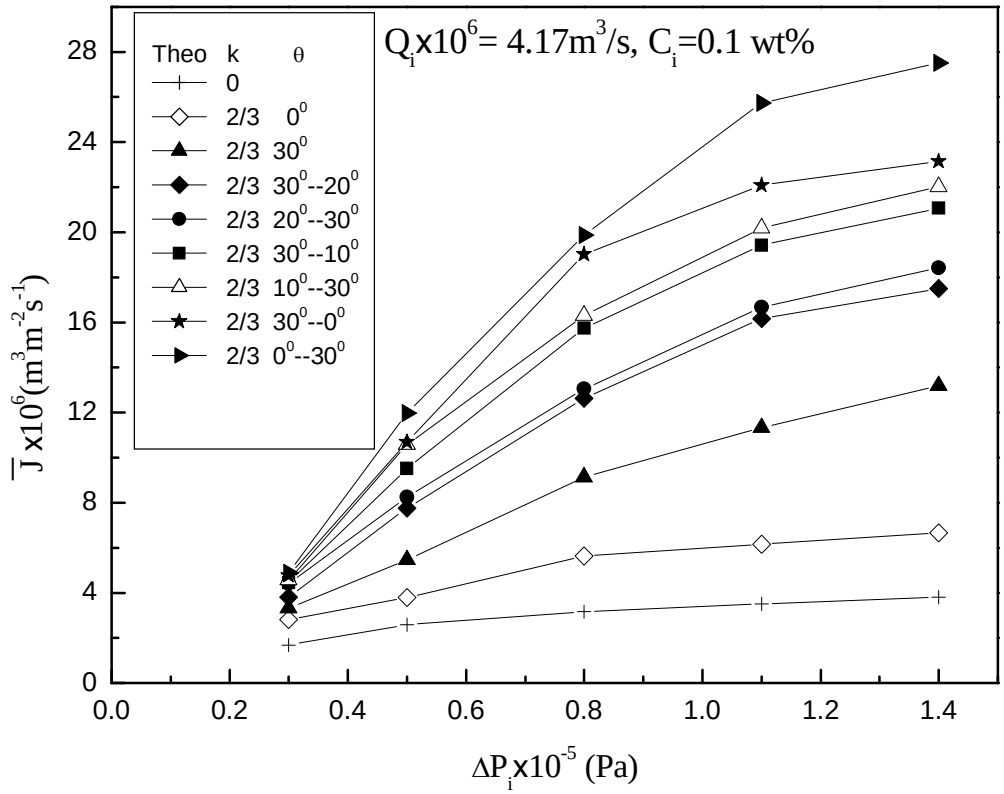
Theo k θ
0
2/3 0⁰
2/3 30⁰
2/3 30⁰--20⁰
2/3 20⁰--30⁰
2/3 30⁰--10⁰
2/3 10⁰--30⁰
2/3 30⁰--0⁰
2/3 0⁰--30⁰
Qix10⁶= 4.17m³/s, Ci=0.1 wt%
J̄ x10⁶(m³m⁻²s⁻¹)
ΔPix10⁻⁵ (Pa)
0
4
8
12
16
20
24
28
0.0
0.2
0.4
0.6
0.8
1.0
1.2
1.4

Fig.4

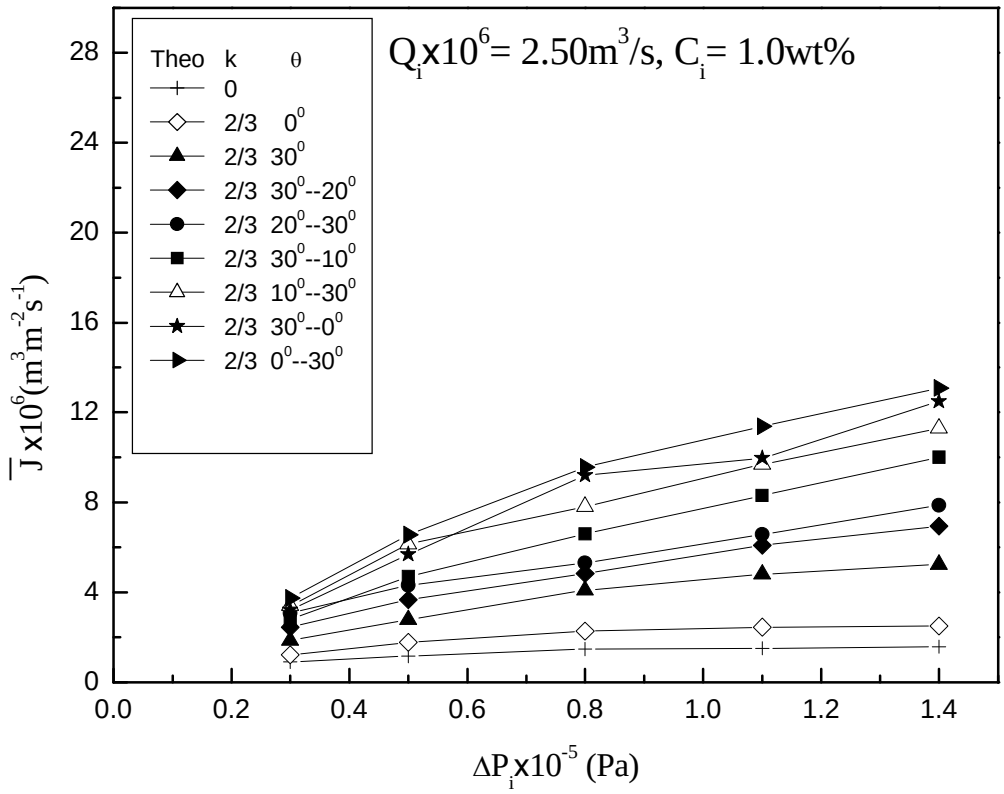
Theo k θ
0
2/3 0⁰
2/3 30⁰
2/3 30⁰--20⁰
2/3 20⁰--30⁰
2/3 30⁰--10⁰
2/3 10⁰--30⁰
2/3 30⁰--0⁰
2/3 0⁰--30⁰
Qix10^6= 2.50m^3/s, Ci= 1.0wt%
J̄ x10^6(m^3m^-2s^-1)
ΔPix10^-5 (Pa)
0
4
8
12
16
20
24
28
0.0
0.2
0.4
0.6
0.8
1.0
1.2
1.4

Fig.5

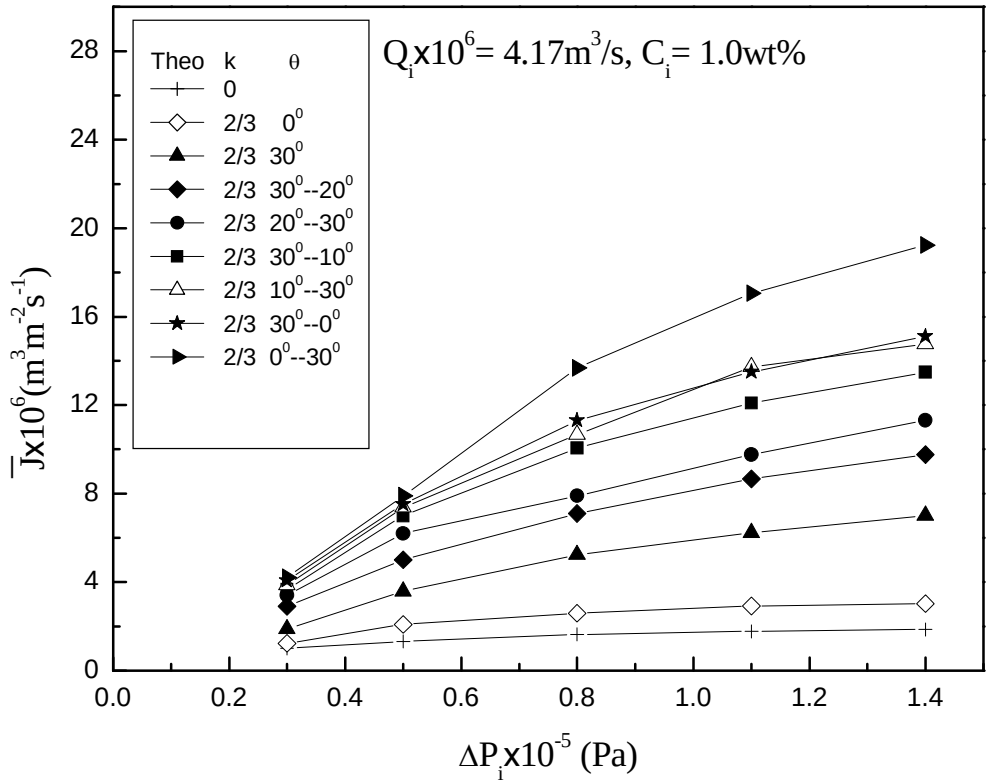
Theo k θ
0
2/3 0⁰
2/3 30⁰
2/3 30⁰--20⁰
2/3 20⁰--30⁰
2/3 30⁰--10⁰
2/3 10⁰--30⁰
2/3 30⁰--0⁰
2/3 0⁰--30⁰
Qix10^6= 4.17m^3/s, Ci= 1.0wt%
J̄x10^6(m^3m^-2s^-1)
ΔPix10^-5 (Pa)
0
4
8
12
16
20
24
28
0.0
0.2
0.4
0.6
0.8
1.0
1.2
1.4

Fig.6

Table 1

Experimental values of ϕ: (a) k=0; (b) k=2/3

	θ	C_i	$\phi \times 10^{-6} (m^2 \cdot s \cdot m^{-3})$			
			$Q_i \times 10^6$	$Q_i \times 10^6$	$Q_i \times 10^6$	$Q_i \times 10^6$
	(deg)	(wt%)	= 1.67 m^3/s	= 2.50 m^3/s	= 3.33 m^3/s	= 4.17 m^3/s
(a)		0.1	0.242	0.219	0.211	0.197
		1.0	0.538	0.498	0.448	0.412
(b)	0	0.1	0.121	0.118	0.092	0.080
	0	1.0	0.352	0.292	0.260	0.238
	30	0.1	0.044	0.049	0.024	0.015
	30	1.0	0.192	0.106	0.074	0.063
	30→20	0.1	0.020	0.019	0.017	0.012
	30→20	1.0	0.108	0.085	0.070	0.057
	20→30	0.1	0.019	0.018	0.016	0.010
	20→30	1.0	0.099	0.078	0.070	0.052
	30→10	0.1	0.019	0.017	0.015	0.010
	30→10	1.0	0.054	0.051	0.038	0.034
	10→30	0.1	0.018	0.016	0.013	0.009
	10→30	1.0	0.050	0.048	0.035	0.026
	30→0	0.1	0.017	0.014	0.012	0.009
	30→0	1.0	0.048	0.045	0.029	0.022
	0→30	0.1	0.014	0.009	0.006	0.006
	0→30	1.0	0.040	0.034	0.020	0.016

Table 2

Experimental values of $\left(R_m + R_f\right)$: (a) k=0; (b) k=2/3

	θ	C_i	$\left(R_m + R_f\right)\times 10^{-10}\left(Pa\cdot m^2\cdot s\cdot m^{-3}\right)$			
			$Q_i \times 10^6$	$Q_i \times 10^6$	$Q_i \times 10^6$	$Q_i \times 10^6$
	(deg)	(wt%)	= 1.67 m^3/s	= 2.50 m^3/s	= 3.33 m^3/s	= 4.17 m^3/s
(a)		0.1	1.125	1.015	0.994	0.941
		1.0	1.911	1.764	1.700	1.678
(b)	0	0.1	1.034	0.923	0.937	0.889
	0	1.0	1.473	1.319	1.293	1.203
	30	0.1	0.885	0.852	0.831	0.842
	30	1.0	1.278	1.143	1.093	1.070
	30→20	0.1	0.770	0.728	0.648	0.546
	30→20	1.0	1.257	0.996	0.801	0.762
	20→30	0.1	0.683	0.656	0.638	0.546
	20→30	1.0	1.208	0.793	0.734	0.559
	30→10	0.1	0.748	0.624	0.509	0.461
	30→10	1.0	1.010	0.767	0.720	0.549
	10→30	0.1	0.652	0.516	0.464	0.431
	10→30	1.0	0.829	0.569	0.581	0.543
	30→0	0.1	0.641	0.515	0.458	0.426
	30→0	1.0	0.787	0.721	0.599	0.526
	0→30	0.1	0.541	0.481	0.432	0.416
	0→30	1.0	0.621	0.589	0.569	0.491